

# Novel Inositol Phospholipid Headgroup Surrogate Crystallized in the Pleckstrin Homology Domain of Protein Kinase B $\alpha$

Stephen J. Mills<sup>†,||</sup>, David Komander<sup>\*,†,||</sup>, Melanie N. Trusselle<sup>†</sup>, Stephen T. Safrany<sup>§</sup>, Daan M. F. van Aalten<sup>‡</sup>, and Barry V. L. Potter<sup>†,\*</sup>

<sup>†</sup>Wolfson Laboratory of Medicinal Chemistry, Department of Pharmacy and Pharmacology, University of Bath, BA2 7AY, U.K., <sup>\*</sup>Division of Biological Chemistry and Molecular Microbiology, School of Life Sciences, University of Dundee, DD1 5EH, U.K., and <sup>§</sup>Department of Pharmacy and Pharmacology, University of Bath, BA2 7AY, U.K., <sup>||</sup>Present address: Institute of Cancer Research, Chester Beatty Laboratories, 237 Fulham Road, London SW3 6JB, U.K., <sup>||</sup>These authors contributed equally to this work.

**ABSTRACT** Protein kinase B (PKB/Akt) plays a key role in cell signaling. The PH domain of PKB binds phosphatidylinositol 3,4,5-trisphosphate translocating PKB to the plasma membrane for activation by 3-phosphoinositide-dependent protein kinase 1. The crystal structure of the headgroup inositol 1,3,4,5-tetrakisphosphate Ins(1,3,4,5)P<sub>4</sub>-PKB complex facilitates *in silico* ligand design. The novel achiral analogue benzene 1,2,3,4-tetrakisphosphate (Bz(1,2,3,4)P<sub>4</sub>) possesses phosphate regiochemistry different from that of Ins(1,3,4,5)P<sub>4</sub> and surprisingly binds with similar affinity as the natural headgroup. Bz(1,2,3,4)P<sub>4</sub> co-crystallizes with the PKB $\alpha$  PH domain in a fashion also predictable *in silico*. The 2-phosphate of Bz(1,2,3,4)P<sub>4</sub> does not interact with any residue, and the  $\nu$ 5-phosphate of Ins(1,3,4,5)P<sub>4</sub> is not mimicked by Bz(1,2,3,4)P<sub>4</sub>. Bz(1,2,3,4)P<sub>4</sub> is an example of a simple inositol phosphate surrogate crystallized in a protein, and this approach could be applied to design modulators of inositol polyphosphate binding proteins.

The protein kinase B (PKB, also known as Akt) subfamily of protein kinases consists of three members (PKB $\alpha$ /Akt1, PKB $\beta$ /Akt2, and PKB $\gamma$ /Akt3) with distinct cellular functions (1–3). The activation mechanism of PKB has been extensively studied (4) and depends on the generation of phosphatidylinositol 3,4,5-trisphosphate (PtdIns(3,4,5)P<sub>3</sub>) from phosphatidylinositol 4,5-bisphosphate (PtdIns(4,5)P<sub>2</sub>) on the plasma membrane by phosphoinositide 3-kinase (5). The pleckstrin homology (PH) domain of PKB binds to PtdIns(3,4,5)P<sub>3</sub>, and this interaction recruits PKB to the plasma membrane (6); PKB is subsequently activated by phosphorylation at two sites (7). The PH domain of PKB can also bind phosphatidylinositol 3,4-bisphosphate (PtdIns(3,4)P<sub>2</sub>) (8–10), and the headgroup derivatives *myo*-inositol 1,3,4,5-tetrakisphosphate (Ins(1,3,4,5)P<sub>4</sub>, **1a** and **1b** in Figure 1) and *myo*-inositol 1,3,4-trisphosphate (Ins(1,3,4)P<sub>3</sub>). Importantly, the 5-phosphate of both PtdIns(3,4,5)P<sub>3</sub> and Ins(1,3,4,5)P<sub>4</sub> is solvent-exposed and not actively contributing to PKB PH domain binding (11). Cellular levels of PtdIns(3,4,5)P<sub>3</sub> are tightly controlled, and PKB activation is negatively regulated by the tumor suppressor phosphatase PTEN (protein phosphatase and tensin homologue deleted on chromosome 10), which dephosphorylates PtdIns(3,4,5)P<sub>3</sub> at the  $\nu$ 3-

position (12). In cells lacking PTEN, PKB is constitutively active, which exerts its anti-apoptotic effects and leads to tumor growth. Therefore, specific PKB inhibitors may deliver a targeted strategy to address patients who suffer from PTEN-induced tumors (13).

Crystal structures of Ins(1,3,4,5)P<sub>4</sub> bound to the PH domains of a number of proteins have been reported; two of these are PKB (11) and 3-phosphoinositide-dependent protein kinase 1 (PDK-1) (14). The design of ligands that interact with PH domains is attractive, potentially providing tools that decouple PtdIns binding from kinase activation. There is a recognized but unmet need to develop simple mimics of inositol polyphosphates (15). Benzene polyphosphates are such molecules, in which the inositol ring is replaced by an aromatic core (16), but their application has never been evaluated in a structural context. Only the phosphates can engage in any flexible movement for benzene polyphosphates; additionally, even this will be different compared to an inositol polyphosphate, and any conformational flexibility derived from the inositol ring will be blocked.

We discovered that benzene 1,2,3,4-tetrakisphosphate (Bz(1,2,3,4)P<sub>4</sub>, **2**) binds to and co-crystallizes with the PH domain of PKB $\alpha$ . Bz(1,2,3,4)P<sub>4</sub> is one of three regioisomeric benzene tetrakisphosphates and was synthesized from 2,3,4-trihydroxybenzaldehyde.

\*Corresponding author,  
b.v.l.potter@bath.ac.uk.

Received for review January 29, 2007  
and accepted March 29, 2007.

Published online April 13, 2007  
10.1021/cb700019r CCC: \$37.00

© 2007 by American Chemical Society

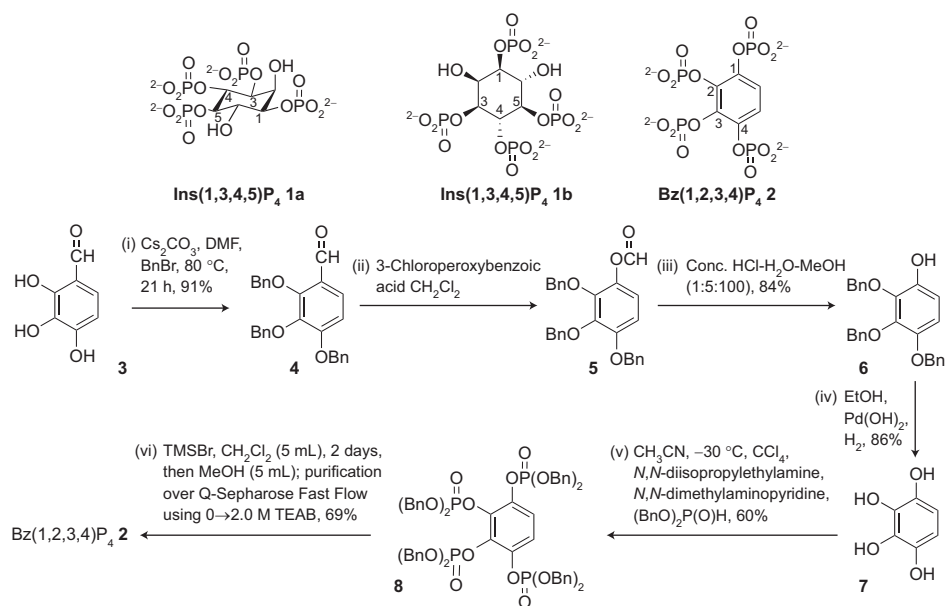


**Figure 1.** *D*-myo-Inositol 1,3,4,5-tetrakisphosphate (1a and 1b) showing the inositol ring pucker and a 2D representation compared to Bz(1,2,3,4)P<sub>4</sub>.

hyde (**3** in Figure 1). Triol **3** was benzylated to afford 2,3,4-tri-*O*-benzyloxybenzaldehyde **4**, which was oxidized to the formate ester **5** and then hydrolyzed to give 2,3,4-tribenzyloxyphenol **6**. The benzyl groups were removed to give 1,2,3,4-tetrahydroxybenzene **7** (17), and the hydroxyl groups were phosphorylated using a modified method initially developed by Silverberg (18) to give compound **8** in 60% yield. The benzyl protecting groups of **8** were deblocked to give the crude product **2**, which was purified over a column of Q-Sepharose Fast Flow using a gradient of triethylammonium bicarbonate buffer to give pure tetrakisphosphate **2** in 69% yield.

Importantly, using quantitative time-resolved FRET (TR-FRET) analysis of the glutathione S-transferase (GST)-tagged PH domain in complex with Eu-chelated anti-GST antibody, biotinylated PtdIns(3,4)P<sub>2</sub>, and streptavidin-coated allophycocyanin (APC) (14), it was found that the pI<sub>C50</sub> for Bz(1,2,3,4)P<sub>4</sub> binding to PKB $\alpha$  is 6.35  $\pm$  0.15 (mean  $\pm$  standard error of the mean

(SEM),  $n = 4$ ), giving a  $K_i$  of 0.08  $\mu$ M (Supplementary Figure 1). For comparison, the natural headgroup Ins(1,3,4,5)P<sub>4</sub> has a pI<sub>C50</sub> of 6.22  $\pm$  0.2 (mean  $\pm$  SEM,  $n = 5$ ) and  $K_i$  value of 0.12  $\mu$ M. The pI<sub>C50</sub> for diC<sub>8</sub>-PtdIns(3,4,5)P<sub>3</sub> is 5.92  $\pm$  0.09 (mean  $\pm$  SEM,  $n = 3$ ), and  $K_i$  is 0.23  $\mu$ M. Since Bz(1,2,3,4)P<sub>4</sub> has good affinity for the PH domain of PKB, it effectively acts as an inositol polyphosphate surrogate.

Crystals of the PKB $\alpha$  PH domain–Bz(1,2,3,4)P<sub>4</sub> complex were grown after mixing purified PKB $\alpha$  PH domain (11) with 10-fold molar excess of Bz(1,2,3,4)P<sub>4</sub>. High-resolution (1.94 Å) diffraction data were collected, and the structure was solved by molecular replacement using the PKB $\alpha$  PH domain–Ins(1,3,4,5)P<sub>4</sub> complex (11) as a search model. Unambiguous  $|F_o| - |F_c|$  electron density for all atoms of the ligand was obtained (Figure 2; Supplementary Table 1). The overall structure of the PKB $\alpha$  PH domain is not significantly different from the previously published structure ( $C_\alpha$  root mean square deviation (rmsd) = 0.55 Å).

However, significant changes are observed in the binding mode of Bz(1,2,3,4)P<sub>4</sub> compared to Ins(1,3,4,5)P<sub>4</sub> (Figure 3, panel a; Supplementary Figure 2). Both ligands occupy the same binding site on the PH domain, and the 1-, 3-, and 4-phosphates of Bz(1,2,3,4)P<sub>4</sub> form a hydrogen bonding pattern to the protein similar to that of the  $\delta$ 1-,  $\delta$ 3-, and  $\delta$ 4-phosphates of Ins(1,3,4,5)P<sub>4</sub> (Supplementary Table 2). The 1/ $\delta$ 1-phosphate is closely enveloped by the Variable Loop-1 region (VL1, residues 16–20), forming similar but not equivalent hydrogen bonds to backbone amide groups of the protein

(Supplementary Table 2). The “fit atoms” alignment tool

was used within Sybyl 7.0 to determine the maximum possible overlap of Bz(1,2,3,4)P<sub>4</sub> and Ins(1,3,4,5)P<sub>4</sub>. The ligands were extracted from the experimental structures, and the equivalent heavy

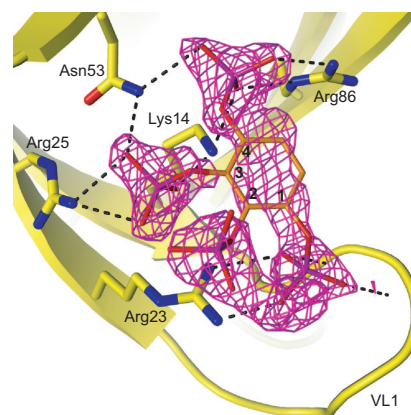


**Figure 2.** Binding of Bz(1,2,3,4)P<sub>4</sub> to the PKB $\alpha$  PH domain in the crystal structure. Unambiguous  $|F_o| - |F_c|$  electron density (magenta), contoured at 2.25 $\sigma$ , is observed, covering all atoms of the ligand. Protein and ligand atoms are colored with purple phosphorus atoms, red oxygen atoms, and blue nitrogen atoms. Hydrogen bonds are indicated as black dotted lines.

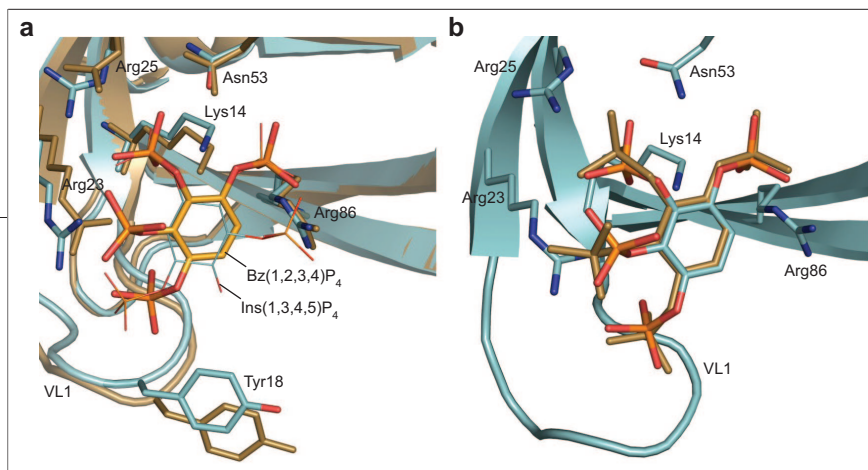


**Figure 3. Superposition of crystallographic and modeled ligands at the PKB $\alpha$  PH domain.** a) Comparison of the crystal structures reveals that the respective phosphorus atoms of the phosphate groups of Ins(1,3,4,5)P $_4$  (line) and Bz(1,2,3,4)P $_4$  (stick) involved in the protein interaction are located within 1.2 Å (1/ $\nu$ 1-phosphate and 3/ $\nu$ 3-phosphate) and 0.3 Å (4/ $\nu$ 4-phosphate) of each other. Interestingly, the PKB $\alpha$  PH domain does not bind to phosphoinositides lacking the  $\nu$ 4-phosphate; furthermore, mutation of Arg86 or Lys14, both of which contact the  $\nu$ 4-phosphate of Ins(1,3,4,5)P $_4$ , block PKB $\alpha$  PH domain ligand binding (11). The observation that the 4-phosphate of Bz(1,2,3,4)P $_4$  is superposing perfectly with the  $\nu$ 4-phosphate of Ins(1,3,4,5)P $_4$ , indicates the relative importance of this phosphate binding site. b) An overlay of the crystal structure Bz(1,2,3,4)P $_4$  (brown) and docked Bz(1,2,3,4)P $_4$  using GOLD (colored by atom types) bound at the PH domain of PKB $\alpha$ .

atoms were aligned using a least squares fit. The lowest rmsd of equivalent atoms (retaining the 1,3,4-trisphosphate regiochemistry) is 1.04 Å, and the aromatic ring remains tilted with respect to the cyclohexane ring (33.2° between the planes created by the two rings). However, when the PH domains are superposed the rmsd between equivalent atoms of Ins(1,3,4,5)P $_4$  and Bz(1,2,3,4)P $_4$  is comparatively high (6.09 Å over heavy atoms only). The 1-, 3-, and 4-phosphates are below the plane of the ring and interact with PKB *via* hydrogen bonds, while the 2-phosphate is above the plane of the ring and does not engage in H-bonding (Supplementary Figure 2). Low energy conformations of Bz(1,2,3,4)P $_4$  (see Supplementary Methods) reveal that the 2- and the 3-phosphates are restricted to opposite faces of the aromatic ring.

Modeling was used to investigate whether the crystallographic binding modes could be reproduced. Ins(1,3,4,5)P $_4$  and Bz(1,2,3,4)P $_4$  were docked into PKB $\alpha$  to assess if the GOLD docking program could predict the crystallographic binding modes of both compounds. The two orientations (crystal structure and docked) were overlaid and their accuracy evaluated (Figure 3, panel b; Supplementary Figure 3). These structures were a good match (rmsd = 1.42 Å over equivalent heavy atoms), and

the docked model could be used for evaluating other potential binding partners and more drug-like molecules. Stereoview diagrams of 1,3,4-trisphosphate regiochemistry for recognition by PKB $\alpha$  PH domain is provided by Bz(1,2,3,4)P $_4$ , with Ins(1,3,4,5)P $_4$  for comparison (Figure 4, panels a and b).

PKB inhibitors are a priority target of the pharmaceutical industry. Most inhibitors target the ATP binding site of the kinase domain and often prove to be non-specific (19, 20). Therefore, small molecules that specifically target the PH domain of PKB should block its membrane localization and hence the conformational change prior to PKB activation (13). The charges of benzene polyphosphates could be masked with acetoxymethyl or pivaloyloxymethyl groups to provide cell-permeable derivatives, enhancing their value as potential modulatory tools for cell biology.

The addition of Ins(1,3,4,5)P $_4$  to full-length PKB in an *in vitro* kinase assay is insufficient to induce PKB activation (21), and whether PKB binds to soluble inositol phosphates *in vivo* is debated (22). Bz(1,2,3,4)P $_4$  has good affinity for the PKB $\alpha$  PH domain, as determined by TR-FRET. Recent data (22) show that Ins(1,3,4,5)P $_4$  could not compete with PtdIns(3,4,5)P $_3$  binding at the PH domain of PKB $\alpha$ , whereas other data show an affinity of 168  $\mu$ M (23). Affinities of 1.5  $\mu$ M

and higher have also been reported (9, 24). There is no explanation for these differences at present; however, inositol phosphates clearly play an important role in regulating proteins with PH domains, for example, phospholipase C (PLC)  $\delta$ 1(25) and PDK-1 localization *in vivo* (14).

We describe the crystal structure of the novel PtdIns(3,4,5)P $_3$  headgroup mimic Bz(1,2,3,4)P $_4$  in complex with the PH domain of PKB $\alpha$  (Figure 2; Supplementary Table 1). Our modeling approaches indicate that the PKB-PH domain provides a robust scaffold for *in silico* ligand design. This is crucial, since more lipid-like derivatives that might directly interfere with PKB activation (similar to PtdIns(3,4,5)P $_3$  ether analogues) may be unsuitable for co-crystallization studies. We also demonstrate that for Bz(1,2,3,4)P $_4$  only the three phosphate groups equivalent to the 1,3,4-trisphosphate are required for binding, correlating with other crystallographic observations. There are many proteins that bind inositol phosphates and phospholipids. Enzyme-resistant benzene polyphosphates could be used to replace inositol polyphosphates in other crystallization experiments where inositol polyphosphates may be modified by proteins such as phosphatases or kinases. Such inositol phosphate surrogates could be structurally tailored for each protein and should provide new tools to inhibit various inositol polyphosphate binding proteins and phosphoinositide modifying enzymes, as we have recently reported (26, 27).

## METHODS

**Chemistry.** Experimental details are similar to those described previously (26).

**Crystallography of PKB $\alpha$  PH Domain in Complex with Bz(1,2,3,4)P $_4$ .** The PKB $\alpha$  PH domain protein was expressed and purified as described previously (11). The triethylammonium salt of Bz(1,2,3,4)P $_4$  was solubilized directly in an 8.5 mg/mL PKB $\alpha$  PH domain solution to achieve a 10-fold molar excess of ligand over protein and incubated on ice for 1 h. Crystals of the protein–ligand complex were grown using the hanging drop vapor diffusion method derived from several conditions similar to those reported for the PKB $\alpha$  PH domain–



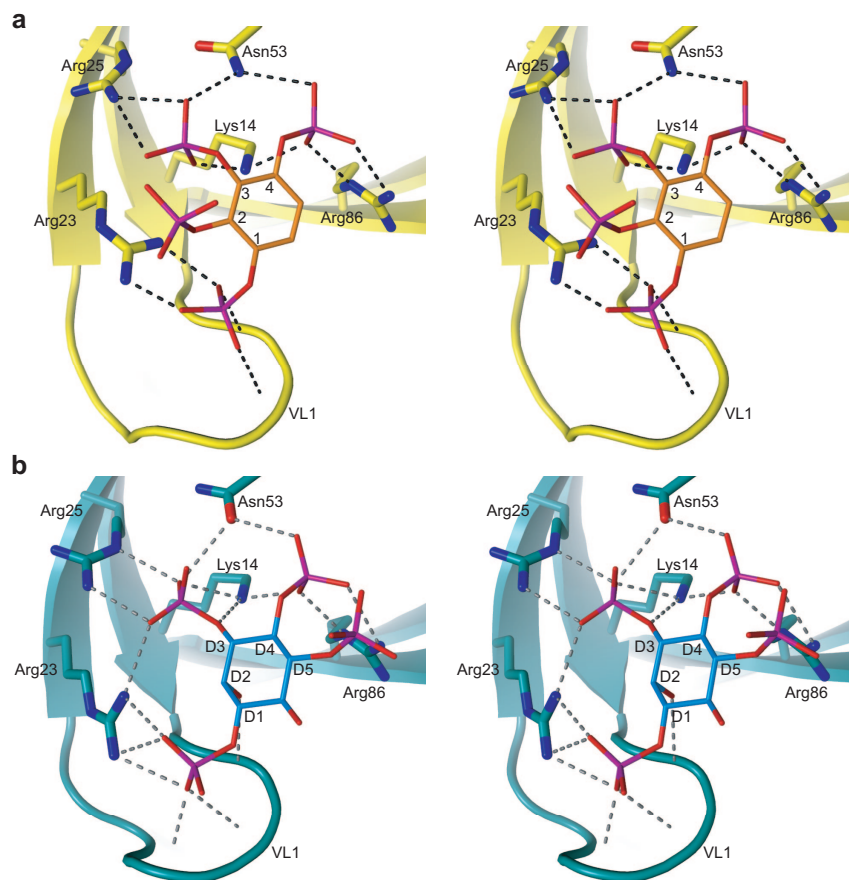


**Figure 4. Hydrogen bonding of PKB $\alpha$  PH domain to InsP $_4$  and BzP $_4$ .** a) Stereoview of Bz(1,2,3,4)P $_4$  bound at the PH domain of PKB $\alpha$ . b) Stereoview of Ins(1,3,4,5)P $_4$  bound at the PH domain of PKB $\alpha$ . Protein and ligand atoms are colored with purple phosphorus atoms, red oxygen atoms, and blue nitrogen atoms. Hydrogen bonds are indicated as dotted lines.

Ins(1,3,4,5)P $_4$  complex (25–30% poly(ethylene glycol) 3000, 0.1 M sodium acetate trihydrate (pH 4.4–5.0), 0.2 M ammonium acetate) (11). Crystals were grown overnight at 20 °C and reached their maximum size after 5 d. Prior to freezing, the crystals were soaked in crystallization solution enriched with 10% 2-methyl-2,4-pentanediol. Diffraction data to a resolution of 1.94 Å were collected at the European Synchrotron Radiation Facility in Grenoble, station ID14, at 100 K, and the structure was solved by rigid body refinement using CNS (28). Subsequently, refinement was carried out in CNS, including extensive simulated annealing to reduce phase bias. Ligand topologies were generated using PRODRG (29). See Supplementary Table 1 for data collection and refinement statistics.

**FRET Binding Experiments.** The GST-tagged PH domain of PKB $\alpha$  was prepared as described in Supplementary Methods. The quantitative TR-FRET analysis of binding was performed in white 96-well

plates (Greiner) using a BMG Labtech PHERAstar with the following settings: excitation 337 nm filter, emission 665 and 620 nm filters, 300 flashes per well, 10  $\mu$ s flashes, read for 400  $\mu$ s following a 50  $\mu$ s delay. Assays were performed in a buffer made of HEPES, 50 mM, pH 6.8; NaCl, 150 mM; MgCl $_2$ , 5 mM; DTT, 5 mM; CHAPS, 0.5%; EDTA, 1 mM in a final assay volume of 50  $\mu$ L.

The  $K_d$  values for biotinylated diC $_8$ -PtdIns(3,4)P $_2$  were determined by increasing amounts (0–100 nM) of biotinylated diC $_8$ -PtdIns(3,4)P $_2$  (Cell Signals), which were incubated with GST-tagged PH domain of PKB $\alpha$  (20 nM) in the presence of excess (21 nM) europium-labeled goat anti-GST antibody (Perkin Elmer) and streptavidin-conjugated APC. The binding of the biotinylated lipid to the protein allows FRET to occur between europium (donor) and APC (acceptor). Fluorescence was monitored at 665 and 620 nm; the ratio of these signals allows the determination of relative amount of binding (Supplemen-

tary Figure 1). The pK $_d$  for biotinylated diC $_8$ -PtdIns(3,4)P $_2$  is 8.23  $\pm$  0.09 (mean  $\pm$  SEM,  $n$  = 3), and  $K_d$  of 5.9 nM. Competition assays were performed with a fixed amount (25 nM) of biotinylated diC $_8$ -PtdIns(3,4)P $_2$  and increasing amounts of Bz(1,2,3,4)P $_4$ , with Ins(1,3,4,5)P $_4$  as a control (Supplementary Figure 1). IC $_{50}$  values were determined, and  $K_i$  values were calculated (30). All curve fitting and statistical analysis was performed using Prism (GraphPad).

#### Synthesis of 2,3,4-Tribenzyloxybenzaldehyde (4).

2,3,4-Trihydroxybenzaldehyde **3** (3.08 g, 20 mmol), cesium carbonate (32.58 g, 100 mmol), and benzyl bromide (11.9 mL, 100 mmol) in dry DMF (100 mL) were stirred for 21 h at 80 °C. The yellow-brown solution was filtered over a bed of Celite and washed with acetone (200 mL). The solvents were evaporated, giving a red-brown oil that was partitioned between CH $_2$ Cl $_2$  and water (200 mL of each). The organic layer was dried, and the solvent was evaporated to give the crude compound. Compound **4** was purified by flash chromatography (CH $_2$ Cl $_2$ ) to give a white solid,  $R_f$  = 0.40 (CH $_2$ Cl $_2$ ), 7.73 g (91%), mp 74–75 °C (hexane).

#### Synthesis of 2,3,4-Tribenzyloxyphenol (6).

3-Chloroperoxybenzoic acid (2.9 g, 16.8 mmol) was added to a solution of 2,3,4-tri-*O*-benzyloxybenzaldehyde **4** (4.245 g, 10 mmol) in dry CH $_2$ Cl $_2$  (100 mL), and the mixture was stirred for 20 h at RT. The organic layer was washed with an aqueous solution of 10% sodium metabisulfite, a saturated solution of sodium hydrogen carbonate (2  $\times$  100 mL of each), and water (100 mL). The organic layer was dried, and the solvent was evaporated to give the crude formate ester **5** as a yellow syrup,  $R_f$  = 0.56 (CH $_2$ Cl $_2$ ). Compound **5** was dissolved in methanol (50 mL) containing 0.5 mL of concentrated HCl and 2.5 mL of water and then stirred for 2 h at RT. The reaction was neutralized using solid NaHCO $_3$  (5 g), the remaining solid was filtered, and the solvent was evaporated. Compound **6** was purified by flash chromatography (CHCl $_3$ ) and isolated as a pale yellow oil,  $R_f$  = 0.40 (CHCl $_3$ ), 3.485 g (84%).

#### Synthesis of 1,2,3,4-Tetrahydroxybenzene (7).

2,3,4-Tribenzyloxyphenol **6** (3.36 g, 8.15 mmol) was dissolved in ethanol (100 mL) followed by the addition of 20% palladium hydroxide (500 mg). The air was expelled from the vessel, and the mixture was stirred over an atmosphere of hydrogen for 24 h at RT. The solution was filtered over a bed of Celite, and the solvent was evaporated giving a beige solid,  $R_f$  = 0.40 (CH $_2$ Cl $_2$ /MeOH 9:1), 993 mg (86%); mp 162 °C (ether/hexane).

#### Synthesis of 1,2,3,4-Tetrakis(dibenzyloxyphosphoryloxy)benzene (8).

Carbon tetrachloride (1.93 mL, 20 mmol), *N,N*-diisopropylethylamine (1.46 mL, 8.4 mmol), a catalytic amount of *N,N*-dimethylaminopyridine (49 mg, 0.40 mmol), and dibenzylphosphite (1.33 mL, 6 mmol) were stirred in dry acetonitrile (30 mL) and cooled using dry ice alone. 1,2,3,4-Tetrahydroxybenzene **7** (142 mg, 1.0 mmol) was added to the solution over 5 min. The solution was stirred for a further 2 h, allowing the reaction to warm to RT. The organic solvent was evaporated, dichloromethane (200 mL) was added and washed with water (200 mL), and

the organic solvent was evaporated. Compound **8** was purified by flash chromatography using ethyl acetate/hexane (1:1) to provide 706 mg (60%) as a colorless syrup,  $R_f = 0.20$  (ether),  $R_f = 0.46$  (EtOAc/hexane 2:1).

**Synthesis of Benzene 1,2,3,4-tetrakisphosphate (2).** Compound **8** (119 mg, 100  $\mu\text{mol}$ ) and bromotrimethylsilane (1.0 mL, 7.58 mmol) were stirred in dry  $\text{CH}_2\text{Cl}_2$  (5 mL) for 2 d under an atmosphere of nitrogen. The solvents were evaporated to give a syrup that was dissolved in methanol (5 mL) and then stirred for 5 min. Compound **2** was purified by ion exchange chromatography over Q-Sepharose Fast Flow using a gradient of TEAB (0  $\rightarrow$  2.0 M) and eluted between 1.1 and 1.8 M buffer to give a glassy triethylammonium salt, 69 mg (69  $\mu\text{mol}$ , 69%).

PyMOL was used to generate all figures.

**Accession Codes:** The coordinates of the PKB $\alpha$  PH domain–Bz(1,2,3,4) $\text{P}_4$  complex have been submitted to the Protein Data Bank and are listed as 2UVM.

**Acknowledgment:** We thank the Wellcome Trust for Programme Grant support (060554 to B.V.L.P) and acknowledge useful discussions with A. M. Riley. Torsten Werner is acknowledged for help in protein production and crystallization. D.K. was supported by a Medical Research Council Predoctoral Fellowship and is now a Beit Memorial Fellow. S.T.S. is a Royal Society University Research Fellow who thanks the Royal Society for financial support. We thank BMG LABTECH for use of their PHERAstar plate reader and G. D. Holman and F. Koumanov (University of Bath) for assistance with TR-FRET assays.

**Supporting Information Available:** This material is available free of charge via the Internet.

## REFERENCES

- Lawlor, M. A., and Alessi, D. R. (2001) PKB/Akt: a key mediator of cell proliferation, survival and insulin responses? *J. Cell Sci.* **114**, 2903–2910.
- Fayard, E., Tintignac, L. A., Baudry, A., and Hemmings, B. A. (2005) Protein kinase B/Akt at a glance. *J. Cell Sci.* **118**, 5675–5678.
- Bellacosa, A., Testa, J. R., Moore, R., and Larue, L. (2004) A portrait of AKT kinases: human cancer and animal models depict a family with strong individualities. *Cancer Biol. Ther.* **3**, 268–275.
- Mora, A., Komander, D., van Aalten, D. M. F., and Alessi, D. R. (2004) PDK1, the master regulator of AGC kinase signal transduction. *Semin. Cell Dev. Biol.* **15**, 161–170.
- Vanhaesebroeck, B., and Alessi, D. R. (2000) The PI3K-PDK1 connection: more than just a road to PKB. *Biochem. J.* **346**, 561–576.
- Andjelkovic, M., Alessi, D. R., Meier, R., Fernandez, A., Lamb, N. J., Frech, M., Cron, P., Cohen, P., Lucocq, J. M., and Hemmings, B. A. (1997) Role of translocation in the activation and function of protein kinase B. *J. Biol. Chem.* **272**, 31515–31524.
- Bayascas, J. R., and Alessi, D. R. (2005) Regulation of Akt/PKB Ser473 phosphorylation. *Mol. Cell* **18**, 143–145.
- Franke, T. F., Kaplan, D. R., Cantley, L. G., and Toker, A. (1997) Direct regulation of the Akt proto-oncogene product by phosphatidylinositol-3,4-bisphosphate. *Science* **275**, 665–668.
- Frech, M., Andjelkovic, M., Ingley, E., Reddy, K. K., Falck, J. R., and Hemmings, B. A. (1997) High affinity binding of inositol phosphates and phosphoinositides to the pleckstrin homology domain of RAC/protein kinase B and their influence on kinase activity. *J. Biol. Chem.* **272**, 8474–8481.
- Rong, S.-B., Hu, Y., Enyedy, I., Powis, G., Meuillett, E. J., Wu, X., Wang, R., Wang, S., and Kozikowski, A. (2001) Molecular modeling studies of the Akt PH domain and its interaction with phosphoinositides. *J. Med. Chem.* **44**, 898–908.
- Thomas, C. C., Deak, M., Alessi, D. R., and van Aalten, D. M. F. (2002) High-resolution structure of the pleckstrin homology domain of protein kinase b/akt bound to phosphatidylinositol (3,4,5)-trisphosphate. *Curr. Biol.* **12**, 1256–1262.
- Leslie, N. R., and Downes, C. P. (2004) PTEN function: how normal cells control it and tumour cells lose it. *Biochem. J.* **382**, 1–11.
- Harris, T. K. (2003) PDK1 and PKB/Akt: ideal targets for development of new strategies to structure-based drug design. *IUBMB Life* **55**, 117–126.
- Komander, D., Fairservice, A., Deak, M., Kular, G. S., Prescott, A. R., Downes, C. P., Safrany, S. T., Alessi, D. R., and van Aalten, D. M. F. (2004) Structural insights into the regulation of PDK1 by phosphoinositides and inositol phosphates. *EMBO J.* **23**, 3918–3928.
- Potter, B. V. L., and Lampe, D. (1995) Chemistry of inositol lipid mediated cellular signaling. *Angew. Chem., Int. Ed. Engl.* **34**, 1933–1972.
- Ward, S. G., Mills, S. J., Liu, C. S., Westwick, J., and Potter, B. V. L. (1995) *D-myo*-inositol 1,4,5-trisphosphate analogues modified at the 3-position inhibit phosphatidylinositol 3-kinase. *J. Biol. Chem.* **270**, 12075–1284.
- Hansen, C. A., Dean, A. B., Draths, K. M., and Frost, J. W. (1999) Synthesis of 1,2,3,4-tetrahydroxybenzene from *D*-glucose: exploiting *myo*-inositol as a precursor to aromatic chemicals. *J. Am. Chem. Soc.* **121**, 3799–3800.
- Silverberg, L. J., Dillon, J. L., and Vemishetti, P. (1996) A simple, rapid and efficient protocol for the selective phosphorylation of phenols with dibenzyl phosphite. *Tetrahedron Lett.* **37**, 771–774.
- Bain, J., McLauchlan, H., Elliott, M., and Cohen, P. (2003) The specificities of protein kinase inhibitors: an update. *Biochem. J.* **371**, 199–204.
- Davies, S. P., Reddy, H., Caivano, M., and Cohen, P. (2000) Specificity and mechanism of action of some commonly used protein kinase inhibitors. *Biochem. J.* **351**, 95–105.
- Alessi, D. R., Deak, M., Casamayor, A., Caudwell, F. B., Morrice, N., Norman, D. G., Gaffney, P., Reese, C. B., MacDougall, C. N., Harbison, D., Ashworth, A., and Bownes, M. (1997) 3-Phosphoinositide-dependent protein kinase-1 (PDK1): structural and functional homology with *Drosophila* DSTPK61 kinase. *Curr. Biol.* **7**, 776–789.
- Downes, C. P., Gray, A., Fairservice, A., Safrany, S. T., Batty, I. H., and Fleming, I. (2005) The regulation of membrane to cytosol partitioning of signalling proteins by phosphoinositides and their soluble head-groups. *Biochem. Soc. Trans.* **33**, 1303–1307.
- Ropars, V., Guichou, J.-F., Auguin, D., Barthe, P., Noguchi, M., and Roumestand, C. (2006) Bases structurales de l'inhibition de la kinase Akt (PKB) par le peptide inhibiteur Akt-in: une étude RMN. *C. R. Chimie* **9**, 439–444.
- Luo, H. R., Huang, Y. E., Chen, J. C., Saiardi, A., Iijima, M., Ye, K., Huang, Y., Nagata, E., Devreotes, P., and Snyder, S. H. (2003) Inositol pyrophosphates mediate chemotaxis in *Dictyostelium* via pleckstrin homology domain-PtdIns(3,4,5) $\text{P}_3$  interactions. *Cell* **114**, 559–572.
- Young, K. W., Garro, M. A., Challiss, R. A. J., and Nahorski, S. R. (2004) NMDA-receptor regulation of muscarinic-receptor stimulated inositol 1,4,5-trisphosphate production and protein kinase C activation in single cerebellar granule neurons. *J. Neurochem.* **89**, 1537–1546.
- Mills, S. J., Dozol, H., Vandeput, F., Backers, K., Woodman, T., Emeux, C., Spiess, B., and Potter, B. V. L. (2006) 3-Hydroxybenzene 1,2,4-trisphosphate, a novel second messenger mimic and unusual substrate for Type-1 *myo*-inositol 1,4,5-trisphosphate 5-phosphatase: synthesis and physicochemistry. *ChemBioChem* **7**, 1696–1706.
- Vandeput, F., Combettes, L., Mills, S. J., Backers, K., Wohlkonig, A., Parys, J. B., De Smedt, H., Missiaen, L., Dupont, G., Potter, B. V. L., and Emeux, C. (2007) Biphenyl 2,3',4,5',6-pentakisphosphate, a novel inositol polyphosphate surrogate, inhibits the activity of two inositol 5-phosphatases and modulates  $\text{Ca}^{2+}$  responses in rat hepatocytes. *FASEB J.* Epub ahead of print; DOI: 10.1096/fj.06-7691com.
- Brunger, A. T., Adams, P. D., Clore, G. M., DeLano, W. L., Gros, P., Grosse-Kunstleve, R. W., Jiang, J. S., Kuszewski, J., Nilges, M., Pannu, N. S., Read, R. J., Rice, L. M., Simonson, T., and Warren, G. L. (1998) Crystallography & NMR system: a new software suite for macromolecular structure determination. *Acta Crystallogr., Sect. D* **54**, 905–921.
- Schuettkopf, A. W., and van Aalten, D. M. F. (2004) PRODRG: a tool for high-throughput crystallography of protein-ligand complexes. *Acta Crystallogr., Sect. D* **60**, 1355–1363.
- Cheng, Y.-C., and Prusoff, W. H. (1973) Relationship between the inhibition constant ( $K_i$ ) and the concentration of inhibitor which causes 50 per cent inhibition ( $I_{50}$ ) of an enzymatic reaction. *Biochem. Pharmacol.* **22**, 3099–3108.
- DeLano, W. L. (2002) *The PyMOL Molecular Graphics System*, DeLano Scientific, San Carlos, CA.